Computer Simulation of Ion Clouds in a Penning Trap

D. H. E. Dubin and T. M. O'Neil

Department of Physics, University of California at San Diego, La Jolla, California 92093
(Received 14 October 1987)

Motivated by recent experiments, a series of molecular-dynamics simulations of ions confined in a Penning trap have been performed. The temperature T and the density n_0 are such that the correlation parameter Γ is large ($\Gamma = e^2/akT$, where $4\pi a^3/3 = n_0$). However, because of the relatively small size of the ion cloud, results differ considerably from previous studies of unbounded systems. The ions form concentric spheroidal shells, but diffuse freely on the shells. As Γ increases, diffusion decreases and a distorted 2D hexagonal lattice forms on the outer shells.

In a recent series of experiments,[1] a collection of N ions (where $N \simeq 100$–1000) were stored in a Penning trap and cooled to very low temperature ($T \simeq 1$–10 mK). One expects these ions to be strongly correlated since the coupling parameter Γ is larger than unity.

The relatively small number of ions used in the experiments makes the system ideal for molecular-dynamics (MD) simulations with realistic boundary conditions. We have performed such simulations for $N = 100$ and $N = 256$ in the large-Γ regime and have seen behavior quite unlike that observed in simulations of an unbounded homogeneous system of ions.[2] These latter simulations predict a liquid phase for $\Gamma \simeq 2$ and a transition to a body-centered cubic lattice for $\Gamma \simeq 170$. In contrast, we observe that at large Γ the system of ions arranges itself into concentric spheroidal shells. However, the ions wander randomly over the surface of the shells. The system might therefore be characterized as a crystal in the direction perpendicular to the shells and as a liquid on the shells; similar behavior is observed in smectic-liquid crystals.[3] As Γ is further increased, diffusion decreases and a 2D hexagonal lattice forms on the outer shells. However, the lattice is imperfect and diffusion persists even for $\Gamma \simeq 300$–400. A 2D hexagonal lattice on cylindrical shells was observed previously by Rahman and Schiffer[4] in a simulation designed to model a system of ions in a storage ring. These authors also considered spherically symmetric potentials as a test of the effect of boundary conditions on their model. While space does not allow for a detailed comparison, their results are consistent with those presented here.

Our MD code is novel in that it is based on guiding-center equations of motion. We will first discuss the advantages and range of applicability of the code, and then we present the results of the simulations.

In the experiments, a strong magnetic field is applied to confine the ion cloud, and this field makes a straightforward simulation difficult by introducing a small time scale and a small length scale: the cyclotron period and the cyclotron radius. To overcome this difficulty, we average out the cyclotron dynamics, replacing the exact

equations of motion by guiding-center equations of motion.[5] The idea here is that for a sufficiently strong magnetic field the cyclotron motion decouples from the motion associated with the collision dynamics. For $\Gamma > 1$, this decoupling requires the cyclotron frequency to be large compared to the plasma frequency. This strong–magnetic-field limit is often achieved in the experiments,[1] and in this case the guiding-center equations of motion provide a good approximation to the exact dynamics of the system. Furthermore, we will see that for N large, the spatial properties of the guiding-center system in equilibrium are the same as those of an equivalent system undergoing exact dynamics.

In the guiding-center approximation the state of each ion is specified by its guiding-center position $\mathbf{x}$ and its velocity U parallel to the magnetic field $\mathbf{B}$. We take $\mathbf{B}$ to be uniform and directed along the z axis of a cylindrical-coordinate system (ρ, ϕ, z). The equations of motion are then

$$d\mathbf{x}_i/dt = (c/B)\mathbf{E}_i \times \hat{\mathbf{z}} + U_i\hat{\mathbf{z}}, \tag{1a}$$

$$dU_i/dt = (e/m)\mathbf{E}_i \cdot \hat{\mathbf{z}}, \tag{1b}$$

where $\mathbf{E}_i = -\partial\Phi/\partial\mathbf{x}_i$ is the electric field acting on ion i and

$$e\Phi(\mathbf{x}_1, \ldots, \mathbf{x}_N) = \sum_{i>j} \frac{e^2}{|\mathbf{x}_i - \mathbf{x}_j|} + \sum_i \tfrac{1}{2} m\omega_z^2(z_i^2 - \rho_i^2/2) \tag{1c}$$

is the potential energy of the ions. The second term in Eq. (1c) is due to the Penning-trap electrodes, and ω_z is the axial bounce frequency for a single particle in the trap. The first term is the electrostatic interaction energy of the ions (diamagnetism and radiation are unimportant). We also assume that the Penning-trap electrodes are far enough from the ion cloud that image charges may be neglected.

Equations (1) can be written in Hamiltonian form and admit two constants of motion: the Hamiltonian itself, $H = \sum_i mU_i^2/2 + e\Phi$, and the canonical angular momen-

tum, $L = eB\sum_i \rho_i^2/2c$. Thus, one expects the long-time average properties of the system to be given by the Gibbs distribution $f = c\exp[-(H + \omega L)/kT]$, where ω is the rotation frequency.[3] (The cloud rotates about the z axis because of $\mathbf{E} \times \mathbf{B}$ and diamagnetic drifts.) To be precise, the distribution for a microcanonical ensemble should be used rather than that for a canonical ensemble, but the two distributions predict average properties which differ only by $O(1/N)$.[3] Such differences are unimportant for the N values used here, even though we are interested in effects associated with boundedness of the cloud.

In the Gibbs distribution the term ωL can be interpreted as the potential energy of ions in a cylinder of uniform negative charge with density $n_0 = \omega B/2\pi ec$. Such a system is referred to as a one-component plasma (OCP); so the spatial part of the Gibbs distribution is the same for both the magnetically confined ions and an OCP confined by background density n_0 and the Penning-trap electrodes.

By using the canonical ensemble with the exact (rather than guiding-center) expressions for H and L,[6] one again finds an equivalence between the distribution for the magnetically confined ions and the distribution for an OCP, but for a slightly shifted background density. In this way, one verifies the large-N equivalence claimed above for the spatial properties in equilibrium of the guiding-center system and the exact system.

In OCP studies, the degree of correlation is specified by the value of the parameter $\Gamma = e^2/akT$. We determine the temperature as a long-time average of the mean kinetic energy [i.e., $T = \langle(1/N)\sum_i mU_i^2\rangle$]. As is the practice in OCP studies, we calculate the Wigner-Seitz radius a in terms of the background density (i.e., $\frac{4}{3}\pi a^3 n_0 = 1$), where n_0 is determined in the simulations from the time average of the rotational frequency [i.e., $n_0 = (B/2\pi ec)\langle\omega\rangle$].

We now consider some details of our computational methods. We have designed a fourth-order Runga-Kutta algorithm and a fourth-order predictor-corrector algorithm, both with variable time step, to compute the ion orbits using Eq. (1). The codes have been tested against one another and have been vectorized to run efficiently on a Cray X-MP computer. In the code, times are normalized to ω_z^{-1} and distances to $(3e^2/m\omega_z^2)^{1/3}$. We typically integrate for times on the order of $10^4\omega_z^{-1}$; in all runs total energy is conserved to better than 1% of the total kinetic energy, and total angular momentum is conserved to 1 part in 10^5.

Typically, we initialize a run by choosing either random initial conditions or positions obtained from some previous run. Positions and velocities are then shifted, if necessary, to remove all center-of-mass motion (the center-of-mass oscillations decouple from the other degrees of freedom). To cool the ions, a small frictional damping force is applied to the parallel motion of each ion, but this damping is turned off and the system is al-

lowed to equilibrate before any averaging is performed. Care is taken to cool slowly so as to avoid metastable states. The values of H and L determine T and $\langle\omega\rangle$, and in general a spheroidal cloud of correlated ions results; however, in order to improve our statistical averaging and to facilitate presentation of results, we have chosen initial conditions to obtain a spherical cloud. Single-particle functions such as the density, T, and $\langle\omega\rangle$ are then determined as functions of spherical radius. As expected from theory, T and $\langle\omega\rangle$ are constant, within error limits. For each value of H and L several initial conditions were used as a test of the repeatability of the simulations, and results for average quantities agree within statistical error.

We now examine the results of a series of runs employing the MD algorithm discussed above. In all cases we have chosen initial conditions to give a spherically symmetric cloud.

First, we discuss average spatial properties for $N = 100$ and $N = 256$ at various values of Γ. These properties are independent of the value of B chosen since, for a given configuration of ions, a change in B simply rescales the value of ω in $H + \omega L$. Thus, to improve the efficiency of the code we take B small so that dynamics parallel and perpendicular to $\mathbf{B}$ are on the same time scale.

We find that for moderate values of Γ (i.e., $\Gamma \approx 2$–100) the density in the cloud as a function of spherical radius exhibits oscillations. The oscillations have maximum amplitude at the edge and decay away towards the center of the cloud. Such behavior has been seen in a similar system at moderate values of Γ, the OCP with an edge.[7] Totsuji has also observed these oscillations in simulations of ions in a Penning trap with $\Gamma = 35$.[8] This oscillatory behavior is a precursor to the formation of crystal planes. As Γ is increased, the oscillations increase in magnitude until the density between peaks goes to zero; for a spherical cloud with $N = 100$ this occurs at $\Gamma \approx 140$ (see Fig. 1). Thus, the ion cloud separates into concentric spheres; for $N = 100$, there are three spheres with 4 ions in the innermost sphere, 26 in the middle sphere, and 70 in the outermost sphere; for $N = 256$, there are four spheres with 6 ions in the innermost sphere, 30 in the next sphere, between 76 and 78 in the next sphere, and between 142 and 144 in the outermost sphere (fluctuations with time in these numbers will be discussed later). The areas under each peak are about equal, implying that the number of ions per unit area in each sphere is the same, being set by the background density n_0. Thus, the number of ions per sphere roughly scales as the surface area of the sphere.

We now turn to the ion configuration within a sphere. In Fig. 2 we display ion positions at a particular time for the outer sphere of the $N = 100$, $\Gamma = 140$ run in spherical polar coordinates. Over short distances, some order is apparent; however, there seems to be no order over longer distances. We confirm this intuition by calculat-
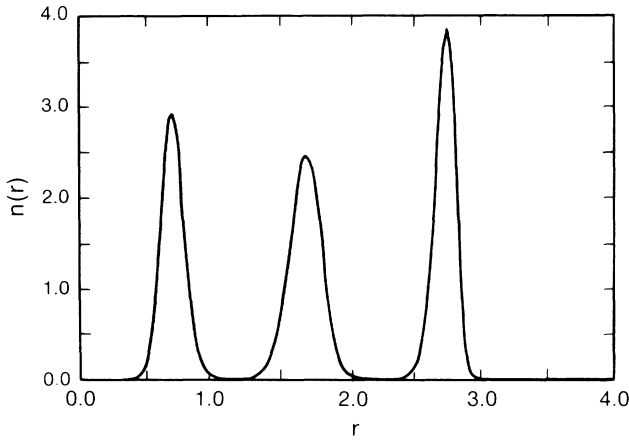
FIG. 1. Density as a function of spherical radius for $N = 100$, $\Gamma = 140$.
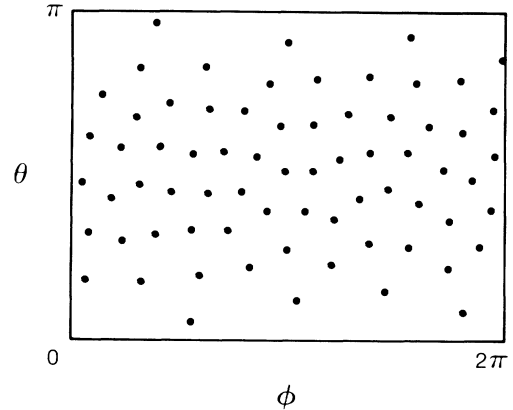
FIG. 2. Polar plot of ion positions for the outermost shell for $N = 100$, $\Gamma = 140$. θ and ϕ measured in radians (ϕ is longitude and θ latitude, measured from pole on positive z axis).

ing the correlation function $c(s)$ of all ions within a particular sphere. The definition of $c(s)$ may be given in terms of the coordination number $C(s)$ through the equation $\int_0^s 2\pi s c(s) = C(s)$, where $C(s)$ is the average number of ions within distance s of an ion at $s = 0$ (counting only ions in the same sphere). We plot $c(s)$ in Fig. 3 for the outermost sphere. For $\Gamma = 140$, $c(s)$ displays decaying oscillations characteristic of a fluid. We study this behavior further by considering the diffusion of the ions. For these studies we take the magnetic field realistically large [i.e., $\omega_z = (0.1 \text{ eV})/mc$], so that the ion dynamics are well represented by guiding-center motion. We calculate the mean square displacement of the ions in time: For distance, we determine $\langle \delta z^2(t) \rangle$ where

$$\langle \delta z^2(t) \rangle = \frac{1}{mN} \sum_{i=1}^{N} \sum_{j=1}^{m} [z_i(t_j + t) - z_i(t_j)]^2,$$

and where $t_j - t_{j-1}$ is constant and $t \le t_j - t_{j-1}$.

This function increases linearly in time for $\langle \delta z^2 \rangle^{1/2}$ small compared to the cloud radius, so that we may obtain the average diffusion coefficient in the z direction through the definition $\langle \delta z^2(t) \rangle = 2D_{zz}t$. For $\Gamma = 140$ this diffusion is shown in Fig. 4 and may be contrasted to a similar plot of $\langle \delta r^2(t) \rangle$ in the same figure (where r is the spherical radius from the center of the cloud). While $\langle \delta z^2(t) \rangle$ does indeed increase linearly, $\langle \delta r^2(t) \rangle$ is almost constant, showing that there is little diffusion of ions from sphere to sphere, while diffusion of ions on the spheres is finite. In fact, at $\Gamma = 140$, ions do sometimes hop from sphere to sphere; however, as Γ is increased, this hopping is not observed. For $N = 256$ some hopping occurs even at $\Gamma \approx 300$; hence the uncertainty in the number of ions in the outer spheres.

Thus, the system behaves like a solid in the radial direction, but like a liquid on each separate sphere. This intermediate state between liquid and solid is quite

FIG. 3. Correlation in the outer sphere for various values of N and Γ. $C(s)$ is also plotted for $N = 256$, $\Gamma = 310$ (dot-dashed curve).
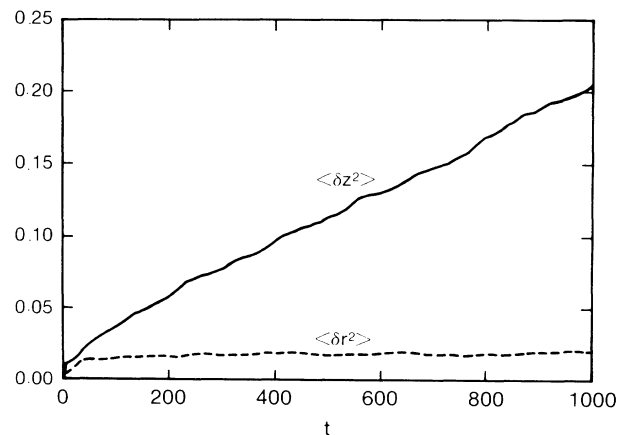
FIG. 4. Mean square change in position vs time for $N = 100$, $\Gamma = 140$: Solid line, $\langle \delta z^2(t) \rangle$; dashed line, $\langle \delta r^2(t) \rangle$.
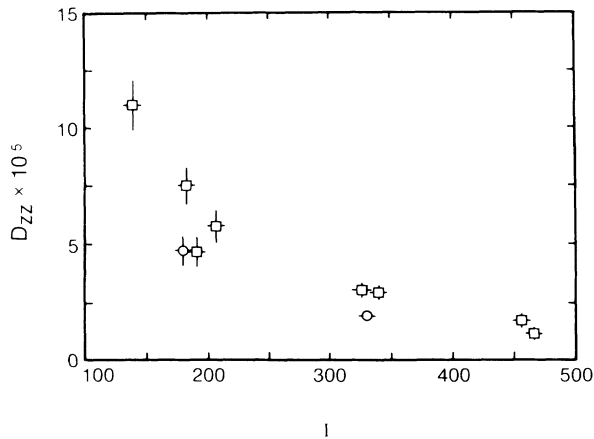
FIG. 5. Average single-particle diffusion in the z direction: Squares, $N = 100$; circles, $N = 256$.

different from anything obtained in previous work on the infinite homogeneous ion system.

Diffusion coefficients at various values of Γ for $N = 100$ and $N = 256$ are displayed in Fig. 5. While diffusion in the z direction decreases with increasing Γ, it is still nonzero for the runs displayed; similarly, correlation functions become more highly peaked as Γ increases but show no abrupt transitions to long-range order. However, as Γ increases, a 2D hexagonal lattice becomes apparent on the spheres. This is most easily seen in Fig.

3, where comparison of $c(s)$ and $C(s)$ shows that the first peak of $c(s)$ contains about 6 ions and the first two peaks about 17–18 ions, corresponding to hexagonal ordering. However, the finite size of the cloud causes imperfections in the lattice and diffusion persists even for large Γ values.

[1]J. Bollinger and D. Wineland, Phys. Rev. Lett. **53**, 348 (1984).

[2]E. Pollock and J. Hansen, Phys. Rev. A **8**, 3110 (1973); W. Slattery, G. Doolen, and H. DeWitt, Phys. Rev. A **21**, 2087 (1980).

[3]L. Landau and E. Lifshitz, *Statistical Physics, Part 1* (Pergamon, Oxford, 1980).

[4]A. Rahman and J. Schiffer, Phys. Rev. Lett. **57**, 1133 (1986).

[5]T. G. Northrop, *The Adiabatic Motion of Charged Particles* (Interscience, New York, 1963).

[6]J. H. Malmberg and T. M. O'Neil, Phys. Rev. Lett. **39**, 1333 (1977).

[7]For a partial listing of papers on the inhomogeneous OCP, see S. Ichimaru, H. Iyetomi, and S. Tanaka, Phys. Rep. **149**, 91 (1987).

[8]H. Totsuji, in *Strongly Coupled Plasma Physics*, edited by F. Rogers and H. Dewitt (Plenum, New York, 1987), p. 19.